

# An Empirical Comparison of Optimizers for Quantum Machine Learning with SPSA-based Gradients

Marco Wiedmann\*, Marc Hölle\*, Maniraman Periyasamy\*, Nico Meyer, Christian Ufrecht, Daniel D. Scherer, Axel Plinge, and Christopher Mutschler  
*Fraunhofer IIS, Fraunhofer Institute for Integrated Circuits IIS, Nuremberg, Germany*

**Abstract**—Variational quantum algorithms (VQAs) have attracted a lot of attention from the quantum computing community for the last few years. Their hybrid quantum-classical nature with relatively shallow quantum circuits makes them a promising platform for demonstrating the capabilities of noisy intermediate scale quantum (NISQ) devices. Although the classical machine learning community focuses on gradient-based parameter optimization, finding near-exact gradients for variational quantum circuits (VQCs) with the parameter-shift rule introduces a large sampling overhead. Therefore, gradient-free optimizers have gained popularity in quantum machine learning circles. Among the most promising candidates is the simultaneous perturbation stochastic approximation (SPSA) algorithm, due to its low computational cost and inherent noise resilience. We introduce a novel approach that uses the approximated gradient from SPSA in combination with state-of-the-art gradient-based classical optimizers. We demonstrate numerically that this outperforms both standard SPSA and the parameter-shift rule in terms of convergence rate and absolute error in simple regression tasks. The improvement of our novel approach over SPSA with stochastic gradient descent (SGD) is even amplified when shot- and hardware-noise are taken into account. We also demonstrate that error mitigation does not significantly affect our results.

**Index Terms**—variational quantum computing, quantum error mitigation, SPSA, gradient free optimization, classical optimizers, quantum regression.

## I. INTRODUCTION

MACHINE learning (ML) has been the key driver for a great variety of recent technological advancements, for example in computer vision [1], natural language processing [2], automatic translation [3], self-driving cars [4], and medical diagnostics [5]. However, machine learning algorithms often require a considerable amount of computational resources and data in the training stage. The rapidly emerging field of quantum machine learning (QML) aims to tackle these challenges by employing a completely different computational paradigm, namely quantum computing.

Quantum computing gained a lot of attention since it offers speedup in terms of computational complexity for a range of

problems, including factoring numbers [6], unstructured search [7], or solving systems of linear equations [8]. Still, the realization of a fault-tolerant quantum computer is yet to be achieved, with current hardware suffering from low qubit counts, coherence times, and high gate- and readout-error rates [9]. As these limitations restrict the size of the quantum circuits that can be executed, the quantum computing community turned to hybrid quantum-classical algorithms, such as variational quantum algorithms (VQAs) [10], in the hope of surpassing classical computing capabilities. They have been applied in the fields of chemistry [11], nuclear physics [12], combinatorial optimization [13], and machine learning [14], which will be the focus of this work.

Like in classical ML, choosing the correct optimizer for the learning task is a key factor in keeping computational costs as low as possible. In the current literature, there are two popular choices. On the one hand, one can either use the parameter-shift rule [15] to evaluate gradients on the quantum hardware and use a gradient-based optimizer, like Adam [16]; on the other hand, one can use gradient-free optimization methods that do not need access to exact derivatives, like simultaneous perturbation stochastic approximation (SPSA) [17]. The latter only requires estimating two expectation values per update step, regardless of the number of parameters that need to be optimized in the circuit. In contrast, the parameter-shift rule requires  $2p$  estimations, where  $p$  is the number of parameters.

In this paper, we present the first quantitative comparison of the following optimizers: (1) Adam, (2) RMSProp, (3) AMS-Grad, (4) SGD, and (5) SGD with momentum in conjunction with the gradients estimated using parameter-shift or SPSA rules. We evaluate each combination of these approaches on multiple regression tasks from the *scikit-learn* library and on real-world data. Numerical experiments were done on the qasm simulator offered by the IBM Quantum services [18]. Both ideal and noisy conditions mimicking the *ibmq\_ehningen* device are employed to study the effect of noise. Additionally, we examine how the use of error mitigation [19] on the noisy simulation impacts the performance of the optimizers.

The paper is structured as follows: Sec. II provides an overview of related literature. The relevant theoretical background is introduced in Sec. III. Sec. III-A introduces vari-

\* These authors contributed equally (name order randomised).

The research is supported by the Bavarian Ministry of Economic Affairs, Regional Development and Energy with funds from the Hightech Agenda Bayern via the project BayQS.  
email address for correspondence: maniraman.periyasamy@iis.fraunhofer.de

ational quantum circuits. Sec. III-B explains how gradients can be estimated on quantum hardware. In Sec. III-C a brief overview of the different optimizers that are used in this paper is given. This is followed by a short high-level introduction to quantum error mitigation in Sec. III-D. A detailed description of numerical experiments is given in Sec. IV and subsequently the results thereof are presented in Sec. V.

## II. RELATED WORK

SGD with SPSA-based gradients (which is just called SPSA in the literature) has recently been compared against other gradient-free and gradient-based optimizers in various settings. The available literature suggests, that SPSA is able to outperform other state-of-the-art gradient-based and gradient-free optimization methods in terms of final error, in a wide range of variational quantum computing tasks like finding energy spectra and ground state energies [20]–[23] or solving linear systems of equations [24], both in noiseless and noisy simulations.

However, the picture is not always that clear. Singh et al. [25] observed, that the SPSA optimizer converged to significantly worse results than all other considered methods when evaluating the ground-state energy and dipole moments of different molecules on a noiseless simulator. While it is affected less by noise than most other optimizers, as can be seen from the improved relative performance to the other methods in the noisy simulation, it is still outperformed by Powell’s method, even in the noisy setting.

The core idea of SPSA, namely approximating gradients by simultaneous perturbations, has also been used to design new optimizers, that are tailored specifically to the training of variational quantum circuits. For example, a quantum version of the natural gradient optimization scheme can be built from a second-order variant of SPSA that approximates the quantum Fischer information matrix [26], [27]. In addition to that, while SPSA does not require the explicit computation of the loss functions gradient, internally it still computes an approximation to it. Therefore it is possible to use the approximated gradient from SPSA with well-established gradient-based optimizers. This idea has been mentioned in [28], but no quantitative comparisons to standard SPSA or the parameter-shift rule are given. While [29] provides such a quantitative comparison, it only considers the stochastic gradient descent (SGD) optimizer.

## III. THEORETICAL BACKGROUND

To give theoretical background, we start by introducing variational quantum circuits (VQCs) and continue by presenting the parameter-shift rule and SPSA. Furthermore, we give a detailed list of the optimizers we examine in this work and close with a look at quantum error mitigation (QEM).

### A. Variational Quantum Circuits

A VQC can be formally described as a sequence of parameterized gates  $U(\mathbf{x}, \boldsymbol{\theta})$ , that prepares a quantum state depending on the initial state  $|\psi_0\rangle$ , input  $\mathbf{x}$  and variational parameters  $\boldsymbol{\theta}$ .

The output is obtained by computing the expectation value of an observable  $A$  [15]

$$f(\mathbf{x}, \boldsymbol{\theta}) := \langle \psi_0 | U^\dagger(\mathbf{x}, \boldsymbol{\theta}) A U(\mathbf{x}, \boldsymbol{\theta}) | \psi_0 \rangle. \quad (1)$$

In the following, we will drop the dependency on the input  $\mathbf{x}$  to facilitate the notation. During the training of this circuit, we want to minimize a loss function  $L(f(\boldsymbol{\theta}), y)$  with respect to some target values  $y$  by tuning the circuit parameters  $\boldsymbol{\theta}$ . For example, this can be realized by iterative gradient descent steps:

$$\hat{\boldsymbol{\theta}}^{k+1} = \hat{\boldsymbol{\theta}}^k - \alpha^k \nabla L(\hat{\boldsymbol{\theta}}^k), \quad (2)$$

where  $\hat{\boldsymbol{\theta}}^k$  denotes the updated parameter vector,  $\alpha^k$  the learning rate and  $\nabla L(\hat{\boldsymbol{\theta}}^k)$  the gradient at iteration  $k$ .

### B. Gradient Computation

In order to determine this gradient, we need to compute partial derivatives  $\partial_{\theta_i} f(\boldsymbol{\theta})$  of the expectation in Eq. (1), which arise due to the chain rule. Since the classical computational cost of computing the unitary  $U$  increases exponentially for larger circuits, it is necessary to obtain gradients directly from the quantum hardware.

1) *Parameter-shift rule:* The parameter-shift rule enables the computation of exact partial derivatives of Eq. (1) from two expectation values per parameter. Following refs. [15] and [30], in order to compute the partial derivative  $\partial_{\theta_i} f(\boldsymbol{\theta})$  with respect to a single parameter  $\theta_i$ , we factor the circuit unitary  $U(\boldsymbol{\theta}) = V\mathcal{G}(\theta_i)W$  into parts, which are constant w.r.t.  $\theta_i$ , and a unitary  $\mathcal{G}(\theta_i)$ , which actually depends on  $\theta_i$ . Furthermore, we assume that  $\mathcal{G}(\theta_i) = e^{-ia\theta_i G}$  with the hermitian generator  $G$  having only two distinct eigenvalues  $e_0$  and  $e_1$ . The parameter-shift rule then states:

$$\partial_{\theta_i} f(\boldsymbol{\theta}) = r [f(\boldsymbol{\theta} + \mathbf{s}) - f(\boldsymbol{\theta} - \mathbf{s})], \quad (3)$$

with  $r = \frac{a}{2}(e_1 - e_0)$  and the components of shift  $\mathbf{s}$  being  $s_i = \frac{\pi}{4r}$  and  $s_j = 0 \forall j \neq i$ .

From this we conclude that  $\partial_{\theta_i} f(\boldsymbol{\theta})$  can be computed directly through two expectation value estimations with shifted parameters. Based on this, the whole gradient can be computed by estimating  $2p$  distinct expectation values, where  $p = |\boldsymbol{\theta}|$  denotes the number of parameters in the trainable circuit.

On quantum hardware, expectation values are formed by averaging noisy measurement outputs over multiple circuit runs, called shots. The finite sampling statistics adversely impacts the computed gradient and therefore the whole training process. In order to get a reliable estimate, multiple shots are required per expectation, making this approach intractable even for medium-sized circuits.

2) *Stochastic Perturbation Simultaneous Approximation:* SPSA is an algorithm designed for circumstances, where only such noisy samples of the loss function are available. It is a gradient-free stochastic optimization algorithm that follows the steepest descent direction on average [31].

To achieve this, the gradient  $\nabla L(\hat{\theta}^k)$  in the parameter update step (cf. Eq. (2)) is replaced by a gradient approximation  $\hat{g}^k(\hat{\theta}^k) \approx \nabla L(\hat{\theta}^k)$ , which is obtained by:

$$\hat{g}^k(\hat{\theta}^k) = \frac{L(\hat{\theta}^k + c^k \Delta^k) - L(\hat{\theta}^k - c^k \Delta^k)}{2c^k} \begin{bmatrix} (\Delta_1^k)^{-1} \\ (\Delta_2^k)^{-1} \\ \vdots \\ (\Delta_p^k)^{-1} \end{bmatrix},$$

where  $c^k$  denotes a small positive scaling factor and  $\Delta^k$  a random perturbation vector at iteration  $k$ . The entries  $\Delta_i^k$  of the perturbation vector are drawn uniformly and independently from the set  $\{-1, 1\}$ .

We observe that all parameters are perturbed at the same time. This means that the gradient approximation can be done by estimating exactly two expectation values, independent of the number of parameters. This can amount to a drastic reduction in training time through computational savings per parameter update step. However, these savings are only effective if they are not canceled out by an overall increase in updates required to reach convergence. Recent work by Kungurtsev et al. suggests, that the overall asymptotic iteration complexity of SPSA is the same as of SGD [32]. They also observe similar convergence rates empirically. This means SPSA can provide real, practical speedup in VQAs.

### C. Optimizers

The way the parameter update is performed based on the estimated or approximated gradient is determined by an optimizer. A very basic optimizer is the gradient descent step from Eq. (2). More sophisticated schemes do not only use the current gradient, but keep a record of gradients from previous iterations  $H^k = \{\nabla L(\hat{\theta}^s)\}_{s=0}^k$  [33]. Formally, they can be expressed as

$$\hat{\theta}^{k+1} = \mathcal{M}(H^k, \phi^k), \quad (4)$$

where the update rule  $\mathcal{M}$  gives the updated parameter vector  $\hat{\theta}^{k+1}$  based on the record  $H^k$  and optimizer hyperparameters  $\phi^k$  e.g. learning rate  $\alpha^k$ .

The optimizers we examine in combination with parameter-shift rule and SPSA are the following.

1) *Stochastic Gradient Descent*: SGD uses the same update rule given in Eq. (2). The stochasticity enters when the gradient is computed over a subset of the training dataset (mini-batches), rather than the entire set.

2) *SGD with momentum*: To accelerate SGD a running mean estimate  $\mu^k$  of the gradient is included, which is updated via

$$\mu^{k+1} = \gamma \mu^k + \nabla L(\hat{\theta}^k).$$

This mean is typically called velocity and is intended to accumulate persistent descent directions across parameter updates

$$\hat{\theta}^{k+1} = \hat{\theta}^k - \alpha^k \mu^{k+1}, \quad (5)$$

where the momentum  $\gamma \in [0, 1]$  is a constant hyperparameter [34].

3) *Adam*: Adaptive moment estimation (Adam) has an individual and adaptive learning rate per parameter, which is based on running estimates of first and second moments

$$\begin{aligned} \mu^{k+1} &= \beta_1 \mu^k + (1 - \beta_1) \nabla L(\hat{\theta}^k) \\ \sigma^{k+1} &= \beta_2 \sigma^k + (1 - \beta_2) \nabla L(\hat{\theta}^k) \odot \nabla L(\hat{\theta}^k), \end{aligned}$$

of the gradient [16]. Here,  $\mu^k$  denotes the mean estimate and  $\sigma^k$  the uncentered variance based on the element-wise square  $\nabla L(\hat{\theta}^k) \odot \nabla L(\hat{\theta}^k)$ .

For a small number of iterations, these estimates are biased due to their initialisation to zero. To compensate this, correction factors are introduced

$$\begin{aligned} \hat{\mu}^{k+1} &= \frac{\mu^{k+1}}{1 - (\beta_1)^{k+1}} \\ \hat{\sigma}^{k+1} &= \frac{\sigma^{k+1}}{1 - (\beta_2)^{k+1}}, \end{aligned}$$

where the decay rates  $\beta_1, \beta_2 \in [0, 1]$  are taken to the  $(k+1)$ -th power. The resulting parameter update is then given by normalizing the mean by the standard deviation  $\sqrt{\hat{\sigma}^{k+1}}$  and subtracting this normalized mean from the current parameters

$$\hat{\theta}^{k+1} = \hat{\theta}^k - \frac{\alpha \hat{\mu}^{k+1}}{\sqrt{\hat{\sigma}^{k+1} + \epsilon}}. \quad (6)$$

Here, the step size  $\alpha$  is a positive scaling factor.

Reddi et al. show that convergence is not generally guaranteed [35]. Nonetheless, Adam is found to be effective in many practical scenarios.

4) *AMSGrad*: This optimizer corrects convergence problems of Adam by maintaining the maximum of the second moment over previous iterations

$$\hat{\sigma}_{\max}^{k+1} = \max(\hat{\sigma}_{\max}^k, \hat{\sigma}^{k+1}),$$

and replacing  $\hat{\sigma}^{k+1}$  in Eq. (6) with this maximum value [35]

$$\hat{\theta}^{k+1} = \hat{\theta}^k - \frac{\alpha \hat{\mu}^{k+1}}{\sqrt{\hat{\sigma}_{\max}^{k+1} + \epsilon}}. \quad (7)$$

5) *RMSProp*: This modified version of SGD with momentum keeps a running estimate of the uncentered variance (mean square)

$$\sigma^{k+1} = \rho \sigma^k + (1 - \rho) \nabla L(\hat{\theta}^k) \odot \nabla L(\hat{\theta}^k),$$

and normalizes the gradient by the standard deviation (root mean square) [36]

$$\mu^{k+1} = \gamma \mu^k + \frac{\alpha^k}{\sqrt{\sigma^{k+1} + \epsilon}} \nabla L(\hat{\theta}^k).$$

### D. Quantum Error Mitigation

A challenge with near-term quantum hardware is its susceptibility to noise. This noise introduces a bias into expectation values, such as in Eq. (1). For ML models based on a VQC this bias should be eliminated as much as possible, since their accuracy depends directly on the estimated expectation.

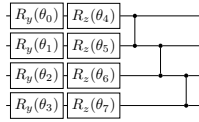


Figure 1. The variational layer of the VQC. Parametrized  $Y$ - and  $Z$ -rotation gates are used to transform the quantum state. A series of  $ZZ$ -gates with nearest-neighbor connectivity is used to create entanglement between qubits. In the full VQC circuit this variational layer is repeated five times. It is preceded by a single encoding layer.

Methods that reduce noise impact are called Quantum Error Mitigation (QEM) [19]. In contrast to Quantum Error Correction (QEC) [37], which currently suffers from a large gate overhead, QEM performs post-processing that does not aim to reduce the effect of noise per shot, but over the whole ensemble of shots. Thus, QEM typically comes with a tradeoff, where for a reduced estimator bias the variance is increased [19]. This can be compensated by an increased number of samples, causing a sampling overhead compared to the ideal noise-free scenario. In this paper, we employ zero-noise extrapolation [38], which uses data gathered from boosted noise levels to extrapolate expectation values to the zero-noise limit. It has already been successfully implemented in different variational algorithms [39]–[42] both in the simulator and on real hardware.

#### IV. METHODS

We conducted numerical experiments to study the performance of different optimizers in training a VQC for multiple regression tasks, where the gradients are either inferred from SPSA or the parameter-shift rule. The following datasets were employed in the experiments:

- The *sklearn* python library features a built-in function *make\_regression* (MReg), which generates the regression target from a random linear combination of the input features with some added gaussian noise.
- Three different four- to five-dimensional artificial datasets first introduced by Friedman [43], [44] (F1, F2, F3). They are built from rational and trigonometric functions of the the input features.
- A real world dataset that captures the relationship of the four ambient variables temperature, air pressure, relative humidity and exhaust vacuum pressure with the power output of a Combined Cycle Power Plant (CCPP) [45].

For each dataset, 500 data points were used for training, 50 for validation, and 100 for model testing. The training was done for a maximum of 30 epochs, with one validation step between each epoch. At the end of the training, the model that attained the best validation results was tested on the test dataset.

The function approximator used for these regression tasks is a VQC consisting of four to five qubits, depending on the feature dimension of the considered dataset, with five repeated variational layers (cf. Fig. 1) and a single observable  $A = Z^{\otimes n}$  estimation constituting the output according to equation

(1). The classical input data was encoded into quantum states with parametrized single-qubit  $X$ -rotations, where the rotation angles are obtained by linearly scaling the feature space into  $[-\pi, \pi]^n$ . The variational parameters were all initialized to zero.

All hyperparameters of the optimizers from section III-C were tuned on each dataset, including the perturbation strength  $c^k$  and learning rate (i.e. a scaling factor applied to each gradient) for the SPSA-based gradient estimation. Since even with SPSA inferred gradients, training the optimizers on the full datasets is computationally expensive, only a subset of 50 randomly sampled points from each dataset were considered for the hyperparameter-tuning.

Since SPSA is often claimed to be especially well suited in noisy settings, it is of prime interest to study the effects of different types of noise, and error mitigation on the optimization procedure. Therefore, the training was done in four different settings. First, an ideal simulation with analytical calculation of all expectation values was performed. Then, shot-noise was taken into account by using a noiseless shot-based simulator with an overall budget of 1024 shots per expectation value estimation. As a next step, realistic hardware noise mimicking the *ibmq\_ehningen* device was added to the simulation. Finally, the experiments were repeated with zero noise extrapolation [38] as a technique to mitigate the hardware noise. For this purpose, we used the native error mitigation capabilities of the IBM Quantum services.

#### V. RESULTS

The results obtained in an ideal, noise-free simulation with the best performing model from the hyperparameter tuning for the SPSA-based gradient estimation step are shown in the top of Table I. Based on the average loss reported in the last row, AMSGrad significantly outperforms SGD, followed closely by Adam and RMSProp when SPSA-based gradients are used. Likewise, the bottom of Table I shows the results obtained during the hyperparameter tuning step of the parameter shift gradient estimation under the same conditions. The average loss shown in Table I already indicates that the parameter-shift based gradient estimation underperforms compared to the SPSA based gradient estimation with all optimizer combinations. However, it should be noted that the hyperparameter results are based on training with 50 data points. Therefore, to validate this observation, we trained all the best performing models again with 500 data points.

Fig. 2 and Fig. 3 show the validation results obtained during training by different optimizers combined with SPSA and parameter-shift based gradient estimation. All curves of the validation results are averaged over five trials and all five datasets. The plots show that the SPSA-based gradient estimation achieves a better solution than the parameter-shift rule in all optimizer combinations. The parameter-shift rule based gradient estimation methods converged to a suboptimal solution and performed two to three times worse than the SPSA-based gradient estimation. On the other hand, the parameter-shift rule requires forty times more circuit simulations per op-

Table I

LOSS AFTER HYPERPARAMETER TUNING FOR EACH DATASET AND OPTIMIZER IN AN IDEAL NOISE-FREE SIMULATION USING SPSA-BASED GRADIENTS (LEFT) AND PARAMETER-SHIFT RULE (RIGHT).

Dataset	SGD	SGD + momentum	Adam	AMSGrad	RMSProp	Dataset	SGD	SGD + momentum	Adam	AMSGrad	RMSProp
MReg	0.17	0.14	0.04	0.02	0.04	MReg	0.23	0.22	0.20	0.21	0.20
CCPP	0.13	0.14	0.11	0.10	0.10	CCPP	0.16	0.32	0.13	0.15	0.13
F1	0.30	0.30	0.16	0.15	0.15	F1	0.30	0.30	0.22	0.24	0.23
F2	0.34	0.26	0.10	0.10	0.14	F2	0.41	0.45	0.38	0.39	0.39
F3	0.22	0.22	0.14	0.12	0.16	F3	0.33	0.36	0.26	0.27	0.26
Average	0.23	0.21	0.11	0.10	0.12	Average	0.29	0.33	0.24	0.25	0.24

timization step compared to SPSA, resulting in high computational costs. The same pattern can be seen in the test results in Table II and Table III. Therefore, no further experiments were performed using the parameter-shift based gradient estimation method. Table II shows that AMSGrad achieves a better solution, followed by Adam and RMSProp within the SPSA-based gradient estimation group. As SGD with Momentum in combination with SPSA converged to a suboptimal solution on the validation curve, it was not tested. From Fig. 2 and Table II, we can infer that AMSGrad, in combination with SPSA, not only converges two to three times faster but also achieves two times better solutions under ideal simulation.

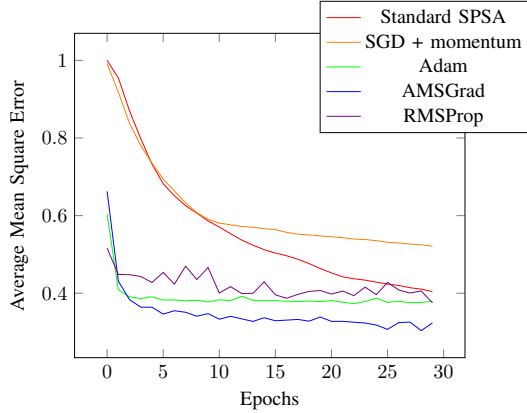


Figure 2. Validation results after every epoch during training on an ideal simulator using SPSA-based gradient estimation

Validation results obtained by different optimizers when simulated on an ideal simulator with shot noise showed similar convergence to ideal simulator results. The test results in Table II show that the performance of all optimizers degrades when shot noise is introduced. However, the standard SPSA and SPSA with RMSProp showed a greater decrease in performance compared to SPSA with Adam or AMSGrad. Next, we repeated the same set of experiments with a noisy simulator simulating the `ibmq_ehningen` noise model. All the optimizers showed similar convergence patterns during training as shown in Fig. 2 and the test results are given in Table II. From Table II, it can be seen that the performance of standard SPSA seems to degrade under different noise conditions, while SPSA with Adam or AMSGrad exhibited a performance similar to its performance under an ideal simulator with shot noise. Finally,

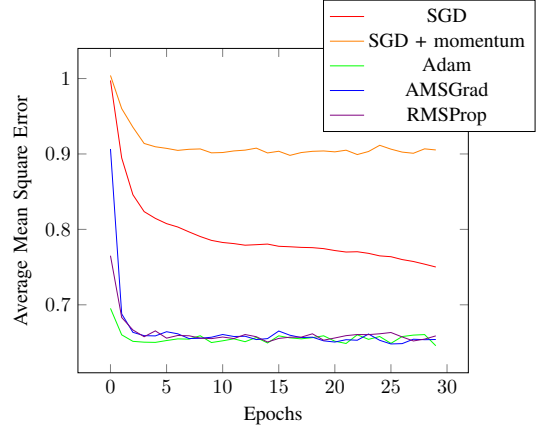


Figure 3. Validation results after every epoch during training on an ideal simulator using parameter-shift rule based gradient estimation

the experiments defined above were repeated with a noisy simulator that simulates the `ibmq_ehningen` noise model and the error mitigation method presented in Section III-D. The test results reported in Table II show again the same hierarchy, with AMSGrad performing the best on average. However, RMSProp achieves almost the same accuracy on average and even surpasses AMSGrad on the F3 dataset. Additionally, it is striking that with the use of error mitigation all methods perform significantly worse than even in the noisy case. A possible explanation for this is the fact that a global observable  $A = Z^{\otimes n}$  was used to constitute the output of the VQC. Kim et al. [42] demonstrated that zero-noise extrapolation performs poorly on global observables.

Throughout all methods used, AMSGrad shows the strongest performance. Adam comes close in terms of performance and requires fewer training steps for some datasets such as CCPP. Generally, both optimizers require drastically fewer training steps until convergence is achieved than standard SPSA and SGD with momentum.

#### A. Generalization on different architecture ansatz

To investigate the dependence of the advantage brought in by AMSGrad on the circuit ansatz, we trained two different VQCs with different circuit ansatzes in the same setting with AMSGrad and the standard SPSA optimizer. Since the difficulty of training the circuit depends strongly on the expressiv-

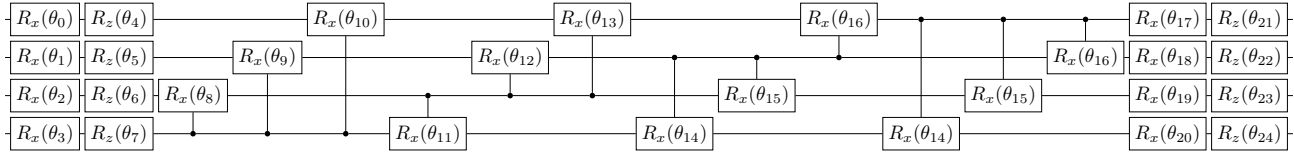


Figure 4. The variational layer of the least expressive VQC proposed by Sim et al.

Table II

SPSA RESULTS. FOR EACH INDIVIDUAL DATASET THE REPORTED LOSS IS THE AVERAGE COMPUTED OVER 5 TRIALS. THE NORMALIZED AVERAGE ERROR WITH RESPECT TO STANDARD SPSA (NORM. AVG.), COMPUTED OVER ALL TRIALS FOR ALL DATASETS, IS GIVEN AT THE BOTTOM OF EACH METHOD.

Method	Dataset	SGD	Adam	AMSGrad	RMSProp
Ideal	MReg	0.0465	0.0317	0.0269	0.0394
	CCPP	0.1034	0.1028	0.1008	0.1036
	F1	0.1587	0.1183	0.1436	0.1449
	F2	0.1327	0.1122	0.0981	0.0841
	F3	0.1440	0.1441	0.1298	0.1559
	Norm. Avg.	1.0000	0.8536	0.8198	0.8958
Shot-based	MReg	0.0492	0.0457	0.0398	0.0546
	CCPP	0.1107	0.1075	0.1049	0.1014
	F1	0.1722	0.1292	0.1391	0.1634
	F2	0.1348	0.1081	0.1146	0.1202
	F3	0.1551	0.1510	0.1328	0.1646
	Norm. Avg.	1.0000	0.8849	0.8540	0.9851
Noisy	MReg	0.0773	0.0537	0.0480	0.0622
	CCPP	0.1219	0.1136	0.0993	0.1070
	F1	0.2441	0.1719	0.1213	0.2126
	F2	0.1620	0.1167	0.1005	0.1218
	F3	0.1762	0.1703	0.1226	0.1655
	Norm. Avg.	1.0000	0.8036	0.6498	0.8492
Error-Mitigated	MReg	0.2080	0.1213	0.0875	0.0885
	CCPP	0.1589	0.1577	0.1343	0.1388
	F1	0.2999	0.1780	0.1972	0.2393
	F2	0.4421	0.2002	0.1800	0.1808
	F3	0.2804	0.2062	0.2162	0.1941
	Norm. Avg.	1.0000	0.6716	0.6203	0.6397

Table III

PARAMETER-SHIFT RULE RESULTS. FOR EACH INDIVIDUAL DATASET THE REPORTED LOSS IS THE AVERAGE COMPUTED OVER 5 TRIALS. THE NORMALIZED AVERAGE ERROR WITH RESPECT TO STANDARD SPSA (NORM. AVG.), COMPUTED OVER ALL TRIALS FOR ALL DATASETS, IS GIVEN AT THE BOTTOM OF EACH METHOD.

Method	Dataset	SGD	Adam	AMSGrad	RMSProp
Ideal	MReg	0.2096	0.2112	0.2071	0.2107
	CCPP	0.2208	0.1271	0.1287	0.1269
	F1	0.2595	0.2352	0.2282	0.2176
	F2	0.3722	0.3784	0.3754	0.3783
	F3	0.3017	0.2795	0.2859	0.2840
	Norm. Avg.	1.0000	0.8866	0.8813	0.8753

ity, the least and most expressive circuits proposed by Sim et al. [46], [47] respectively were chosen to validate the performance of AMSGrad in combination with SPSA-based gradient estimation. Fig. 5 represents one variational layer of the least expressive circuit, and Fig. 4 represents one variational layer of the most expressive circuit. Five such layers were repeated in each VQC. The results shown in Table IV validate that the combination of AMSGrad with SPSA-based gradient estimation yields superior results compared to the standard SPSA method, irrespective of the expressivity of the circuit.

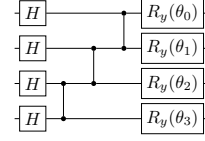


Figure 5. The variational layer of the least expressive VQC proposed by Sim et al.

Table IV

PERFORMANCE OF AMSGRAD AND SPSA ON CIRCUITS WITH DIFFERENT EXPRESSIVITY

Circuit	Dataset	SGD	AMSGrad
Least Expressive circuit	MReg	0.2166	0.0453
	CCPP	0.1406	0.1142
	F1	0.2839	0.1671
	F2	0.5589	0.1287
	F3	0.5147	0.1652
	Norm. Avg.	1.0000	0.4322
Most Expressive circuit	MReg	0.2192	0.0920
	CCPP	0.2353	0.1236
	F1	0.3099	0.2933
	F2	0.5600	0.1533
	F3	0.5483	0.5149
	Norm. Avg.	1.000	0.6208

## VI. CONCLUSION

This paper proposes an optimization scheme for variational quantum circuits by combining the gradient estimate obtained from simultaneous perturbation stochastic approximation with gradient-based optimizers like SGD, Adam, AMSGrad, or RMSProp. We demonstrate with noiseless simulations on simple regression tasks that using the SPSA-approximated gradient improves both the convergence rate by a factor of three and the final absolute error by a factor of more than two compared to the parameter-shift rule. We further observe that the combined SPSA-AMSGrad optimizer consistently outperforms all other methods, including standard SPSA.

Adam, AMSGrad, and RMSProp clearly outperform SGD for SPSA-inferred gradients when considering shot- and hardware noise. The gap in performance grows to a factor of 1.5 for the full noise model. The performance boost between methods remains the same even when error mitigation addresses the hardware noise.

We conclude that combining the computationally cheap to obtain gradient estimate of SPSA with modern gradient-based optimizers drastically speeds up the training process of VQCs and leads to improved convergence.

## REFERENCES

- [1] A. Voulodimos, N. Doulamis, A. Doulamis, E. Protopapadakis *et al.*, “Deep learning for computer vision: A brief review,” *Computational intelligence and neuroscience*, vol. 2018, 2018.
- [2] D. W. Otter, J. R. Medina, and J. K. Kalita, “A survey of the usages of deep learning for natural language processing,” *IEEE transactions on neural networks and learning systems*, vol. 32, no. 2, pp. 604–624, 2020.
- [3] A. Vaswani, N. Shazeer, N. Parmar, J. Uszkoreit, L. Jones, A. N. Gomez, Ł. Kaiser, and I. Polosukhin, “Attention is all you need,” *Advances in neural information processing systems*, vol. 30, 2017.
- [4] A. Baheri, S. Nageshrao, H. E. Tseng, I. Kolmanovsky, A. Girard, and D. Filev, “Deep reinforcement learning with enhanced safety for autonomous highway driving,” in *2020 IEEE Intelligent Vehicles Symposium (IV)*. IEEE, 2020, pp. 1550–1555.
- [5] M. Fatima, M. Pasha *et al.*, “Survey of machine learning algorithms for disease diagnostic,” *Journal of Intelligent Learning Systems and Applications*, vol. 9, no. 01, p. 1, 2017.
- [6] P. W. Shor, “Algorithms for quantum computation: discrete logarithms and factoring,” in *Proceedings 35th annual symposium on foundations of computer science*. IEEE, 1994, pp. 124–134.
- [7] L. K. Grover, “A fast quantum mechanical algorithm for database search,” in *Proceedings of the twenty-eighth annual ACM symposium on Theory of computing*, 1996, pp. 212–219.
- [8] A. W. Harrow, A. Hassidim, and S. Lloyd, “Quantum algorithm for linear systems of equations,” *Physical review letters*, vol. 103, no. 15, p. 150502, 2009.
- [9] J. Preskill, “Quantum computing in the nisq era and beyond,” *Quantum*, vol. 2, p. 79, 2018.
- [10] M. Cerezo *et al.*, “Variational quantum algorithms,” *Nature Reviews Physics*, vol. 3, no. 9, pp. 625–644, 2021.
- [11] P. J. O’Malley, R. Babbush, I. D. Kivlichan, J. Romero, J. R. McClean, R. Barends, J. Kelly, P. Roushan, A. Tranter, N. Ding *et al.*, “Scalable quantum simulation of molecular energies,” *Physical Review X*, vol. 6, no. 3, p. 031007, 2016.
- [12] O. Kiss, M. Grossi, P. Lougovski, F. Sanchez, S. Vallecorsa, and T. Papenbrock, “Quantum computing of the li 6 nucleus via ordered unitary coupled clusters,” *Physical Review C*, vol. 106, no. 3, p. 034325, 2022.
- [13] E. Farhi, J. Goldstone, and S. Gutmann, “A quantum approximate optimization algorithm,” *arXiv preprint arXiv:1411.4028*, 2014.
- [14] E. Farhi and H. Neven, “Classification with quantum neural networks on near term processors,” *arXiv preprint arXiv:1802.06002*, 2018.
- [15] M. Schuld, V. Bergholm, C. Gogolin, J. Izaac, and N. Killoran, “Evaluating analytic gradients on quantum hardware,” *Physical Review A*, vol. 99, no. 3, p. 032331, 2019.
- [16] D. P. Kingma and J. Ba, “Adam: A method for stochastic optimization,” *arXiv preprint arXiv:1412.6980*, 2014.
- [17] J. Spall, “Multivariate stochastic approximation using a simultaneous perturbation gradient approximation,” *IEEE Transactions on Automatic Control*, vol. 37, no. 3, pp. 332–341, 1992.
- [18] “IBM quantum,” <https://quantum-computing.ibm.com/>, 2023.
- [19] Z. Cai, R. Babbush, S. C. Benjamin, S. Endo, W. J. Huggins, Y. Li, J. R. McClean, and T. E. O’Brien, “Quantum error mitigation,” *arXiv preprint arXiv:2210.00921*, 2022.
- [20] N. Sá, I. S. Oliveira, and I. Roditi, “Towards solving the bcs hamiltonian gap in near-term quantum computers,” *Results in Physics*, vol. 44, p. 106131, 2023.
- [21] X. Bonet-Monroig, H. Wang, D. Vermetten, B. Senjean, C. Moussa, T. Bäck, V. Dunjko, and T. E. O’Brien, “Performance comparison of optimization methods on variational quantum algorithms,” *Physical Review A*, vol. 107, no. 3, p. 032407, 2023.
- [22] M. Oliv, A. Matic, T. Messerer, and J. M. Lorenz, “Evaluating the impact of noise on the performance of the variational quantum eigensolver,” *arXiv preprint arXiv:2209.12803*, 2022.
- [23] I. Miháliková, M. Friák, M. Pivoluska, M. Plesch, M. Saip, and M. Šob, “Best-practice aspects of quantum-computer calculations: A case study of the hydrogen molecule,” *Molecules*, vol. 27, no. 3, p. 597, 2022.
- [24] A. Pellow-Jarman, I. Sinayskiy, A. Pillay, and F. Petruccione, “A comparison of various classical optimizers for a variational quantum linear solver,” *Quantum Information Processing*, vol. 20, no. 6, p. 202, 2021.
- [25] H. Singh, S. Mishra, and S. Majumder, “Benchmarking of different optimizers in the variational quantum algorithms for applications in quantum chemistry,” *arXiv preprint arXiv:2208.10285*, 2022.
- [26] J. Gacon, C. Zoufal, G. Carleo, and S. Woerner, “Simultaneous perturbation stochastic approximation of the quantum fisher information,” *Quantum*, vol. 5, p. 567, 2021.
- [27] J. Gidi, B. Candia, A. Muñoz-Moller, A. Rojas, L. Pereira, M. Muñoz, L. Zambrano, and A. Delgado, “Stochastic optimization algorithms for quantum applications,” *arXiv preprint arXiv:2203.06044*, 2022.
- [28] S. Ebadi, A. Keesling, M. Cain, T. T. Wang, H. Levine, D. Bluvstein, G. Semeghini, A. Omran, J.-G. Liu, R. Samajdar *et al.*, “Quantum optimization of maximum independent set using rydberg atom arrays,” *Science*, vol. 376, no. 6598, pp. 1209–1215, 2022.
- [29] T. Hoffmann and D. Brown, “Gradient estimation with constant scaling for hybrid quantum machine learning,” *arXiv preprint arXiv:2211.13981*, 2022.
- [30] G. E. Crooks, “Gradients of parameterized quantum gates using the parameter-shift rule and gate decomposition,” *arXiv preprint arXiv:1905.13311*, 2019.
- [31] J. C. Spall, “An overview of the simultaneous perturbation method for efficient optimization,” *Johns Hopkins apl technical digest*, vol. 19, no. 4, pp. 482–492, 1998.
- [32] V. Kungurtsev, G. Korpas, J. Marecek, and E. Y. Zhu, “Iteration complexity of variational quantum algorithms,” *arXiv preprint arXiv:2209.10615*, 2022.
- [33] D. Choi, C. J. Shallue, Z. Nado, J. Lee, C. J. Maddison, and G. E. Dahl, “On empirical comparisons of optimizers for deep learning,” *arXiv preprint arXiv:1910.05446*, 2019.
- [34] I. Sutskever, J. Martens, G. Dahl, and G. Hinton, “On the importance of initialization and momentum in deep learning,” in *International conference on machine learning*. PMLR, 2013, pp. 1139–1147.
- [35] S. J. Reddi, S. Kale, and S. Kumar, “On the convergence of adam and beyond,” *arXiv preprint arXiv:1904.09237*, 2019.
- [36] T. Tieleman, G. Hinton *et al.*, “Lecture 6.5-rmsprop: Divide the gradient by a running average of its recent magnitude,” *COURSERA: Neural networks for machine learning*, vol. 4, no. 2, pp. 26–31, 2012.
- [37] D. A. Lidar and T. A. Brun, *Quantum error correction*. Cambridge university press, 2013.
- [38] K. Temme, S. Bravyi, and J. M. Gambetta, “Error mitigation for short-depth quantum circuits,” *Physical review letters*, vol. 119, no. 18, p. 180509, 2017.
- [39] A. Kandala, K. Temme, A. D. Córcoles, A. Mezzacapo, J. M. Chow, and J. M. Gambetta, “Error mitigation extends the computational reach of a noisy quantum processor,” *Nature*, vol. 567, no. 7749, pp. 491–495, 2019.
- [40] Y. Li and S. C. Benjamin, “Efficient variational quantum simulator incorporating active error minimization,” *Physical Review X*, vol. 7, no. 2, p. 021050, 2017.
- [41] E. F. Dumitrescu *et al.*, “Cloud quantum computing of an atomic nucleus,” *Physical review letters*, vol. 120, no. 21, p. 210501, 2018.
- [42] Y. Kim, C. J. Wood, T. J. Yoder, S. T. Merkel, J. M. Gambetta, K. Temme, and A. Kandala, “Scalable error mitigation for noisy quantum circuits produces competitive expectation values,” *Nature Physics*, pp. 1–8, 2023.
- [43] J. H. Friedman, “Multivariate adaptive regression splines,” *The annals of statistics*, vol. 19, no. 1, pp. 1–67, 1991.
- [44] L. Breiman, “Bagging predictors,” *Machine learning*, vol. 24, pp. 123–140, 1996.
- [45] P. Tüfekçi, “Prediction of full load electrical power output of a base load operated combined cycle power plant using machine learning methods,” *International Journal of Electrical Power & Energy Systems*, vol. 60, pp. 126–140, 2014.
- [46] S. Sim, P. D. Johnson, and A. Aspuru-Guzik, “Expressibility and entangling capability of parameterized quantum circuits for hybrid quantum-classical algorithms,” *Advanced Quantum Technologies*, vol. 2, no. 12, p. 1900070, 2019.
- [47] T.-A. Drăgan, M. Monnet, C. B. Mendl, and J. M. Lorenz, “Quantum reinforcement learning for solving a stochastic frozen lake environment and the impact of quantum architecture choices,” *arXiv preprint arXiv:2212.07932*, 2022.